Charge-exchange cross sections for 445-MeV Cl ions in solid C targets

C. J. Sofield
Nuclear Physics Division, Atomic Energy Research Establishment, Harwell, United Kingdom Atomic Energy Authority Didcot, Oxfordshire 0X11 ORA, United Kingdom

L. B. Bridwell
Southwest Missouri State University, Springfield, Missouri 65804

C. D. Moak, P. D. Miller, D. C. Gregory, C. M. Jones, G. D. Alton, and P. L. Pepmiller
Oak Ridge National Laboratory, Oak Ridge, Tennessee 37831

J. M. Hall
Kansas State University, Manhattan, Kansas 66506

(Received 24 April 1987; revised manuscript received 30 January 1989)

Nonequilibrium charge-state fractions of ^{35}Cl ions traversing solid C targets have been measured. Absolute intensities of x rays were measured for transitions between various states of the nearly fully stripped ^{35}Cl ions that had an energy of 445 MeV and a velocity of 12.7 MeV/u. An analysis of the data has provided estimates of a number of cross sections for electron capture, excitation, and electron loss of the projectiles. Reasonable agreement has been found between some of these experimental values and theoretical estimates.

I. INTRODUCTION

The theoretical study of electron capture by fast bare nuclei interacting with various targets has received considerable attention in the last few years, particularly those aspects of theory intended to extend calculations to regimes unsuitable to the Oppenheimer-Brinkman-Kramers (OBK) approximation. A considerable amount of this work has been reviewed by Belkic *et al.*[1] and Greenland.[2] There has also been an equivalent interest in theoretical methods of calculating electron loss and excitation of fast projectiles, particularly H-like ions in collisions with various target atoms.[3] In the regime of high projectile charge these theories have not been widely tested. We describe in this paper experimental results for various electron capture, electron loss, and excitation cross sections of ^{35}Cl $Z=17$ ions colliding with carbon atoms.

To achieve a velocity sufficient to produce predominantly fully stripped and H-like ^{35}Cl ions the coupled tandem cyclotron at the Holifield Heavy-Ion Research Facility (HHIRF), Oak Ridge National Laboratory, was used to provide 445-MeV ^{35}Cl ions. Empirical stripping criteria[4] suggested this energy would be sufficient for this purpose. Measurements of the charge-state populations and absolute intensities of the x rays emitted after passing through thin targets were measured. The targets were in fact thin enough to achieve single collision conditions for ground-state capture in $^{35}Cl^{17+}$ and for ground state capture and loss processes in $^{35}Cl^{16+}$.

II. EXPERIMENTAL TECHNIQUE

A. Methodology

The determination of cross sections for the various electron-capture, electron-loss, and excitation processes that take place when a projectile traverses a thin target are based on solving coupled differential equations which are given formally by

$$\frac{d\phi_i}{dx}=\sum_{j\neq i}(\phi_j\sigma_{ji}-\phi_i\sigma_{ij}) , \quad (1)$$

where ϕ_i is the population fraction of ions in state i, σ_{ij} is the cross section for a transition from state i to state j, and x is the target thickness expressed in atoms per unit area. In our case we have chosen a sufficiently high energy to obtain $^{35}Cl^{17+}$, $^{35}Cl^{16+}$ and $^{35}Cl^{15+}$ as the dominant fractions. In addition, the excited states of the hydrogenlike $^{35}Cl^{16+}$ ion and the heliumlike $^{35}Cl^{15+}$ ion could all be populated, in principle. Thus the set of Eqs. (1) has an infinite number of terms. It is expected on theoretical grounds,[5] and from an extrapolation of previous experience,[6] that only the $^{35}Cl^{16+}$ and $^{35}Cl^{15+}$ low-lying excited states will be strongly populated so that Eqs. (1) become tractable. The problems involved in determining the population of the ion and excited state fractions that contribute significantly are thus central to this experimental study. Electrostatic charge state separation and x-ray spectroscopic measurements are adequate tools for this purpose.

Following the work of Allison[7] and the analysis of Eqs. (1) by Datz *et al.*[8] it is important to produce targets thin enough to approach single collision conditions. This maximizes sensitivity to a particular σ_{ij}. Since $\phi_j=1$, Eqs. (1) reduce to

$$\frac{d\phi_i}{dx}\simeq\sigma_{ij} . \quad (2)$$

This requires the production of pure incident beams of each ϕ_j involved in the process.

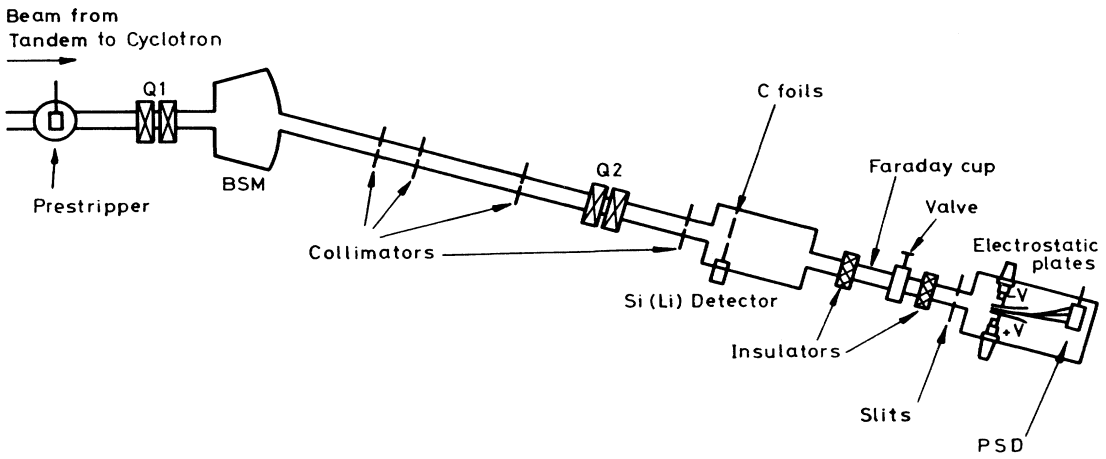

FIG. 1. Schematic of the experimental apparatus. See text for definition of the abbreviations.

B. Target preparation and thickness determination

Thin self-supporting carbon foils were produced by evaporating C in an arc discharge[9] onto glass slides coated with a release agent (RBS 25 detergent[10]). The thickness of the C foils was monitored in the usual way with a quartz-crystal oscillator during deposition. However, more accurate thickness determinations were made on the thicker foils by measuring the energy loss of 5.8-MeV α particles from a thin ^{244}Cm source, and using dE/dx values from Ziegler's tabulations.[11] Thick foil values were used to check measurements of thickness using the elastic recoil detection analysis (ERDA) technique[12] which was extended to the thinnest foils and which also provided light element impurity estimates. Heavy impurities were examined by microbeam proton-induced x-ray emission (PIXE) analysis and foil uniformity examined by concurrent microbeam Rutherford backscattering (RBS) spectrometry determinations.[13]

Impurity levels were estimated to be 0.1 at. % for heavy elements, 3 at. % for O and 8 at. % for H. Following the discussion of the consequences of foil impurities on the cross-section measurements given by Woods[14] we conclude that the impurity levels found in these foils will not significantly affect our results. Note that the O and heavy-element contamination (e.g., Si, K, and Cu) is most likely at the surface of the foil that was in contact with the release agent. We were careful to ensure that the likely contaminated surface was always placed in the upstream side relative to the incident beam which is thus only slightly modified on entry to the target.

C. Charge-state measurements

Charge-state distributions were determined for a range of C foil thicknesses by the usual procedure[15] of electrostatic separation of the ions downstream of the target and detecting the resultant spatially separated charge states using a position sensitive solid-state detector (PSD). A diagram of the apparatus is shown in Fig. 1. A beam of about 50 nA of ^{35}Cl ions was extracted from the HHIRF coupled tandem cyclotron accelerator system and passed through a C prestripper foil (50 or 100 μg/cm^2) to produce the desired range of incident charge states. The required incident charge state was selected with the beam switching magnet (BSM) and focussed via quadrupole elements $Q1$ and $Q2$ onto the C target foil. The magnet (BSM) also determined the beam energy, in this case,

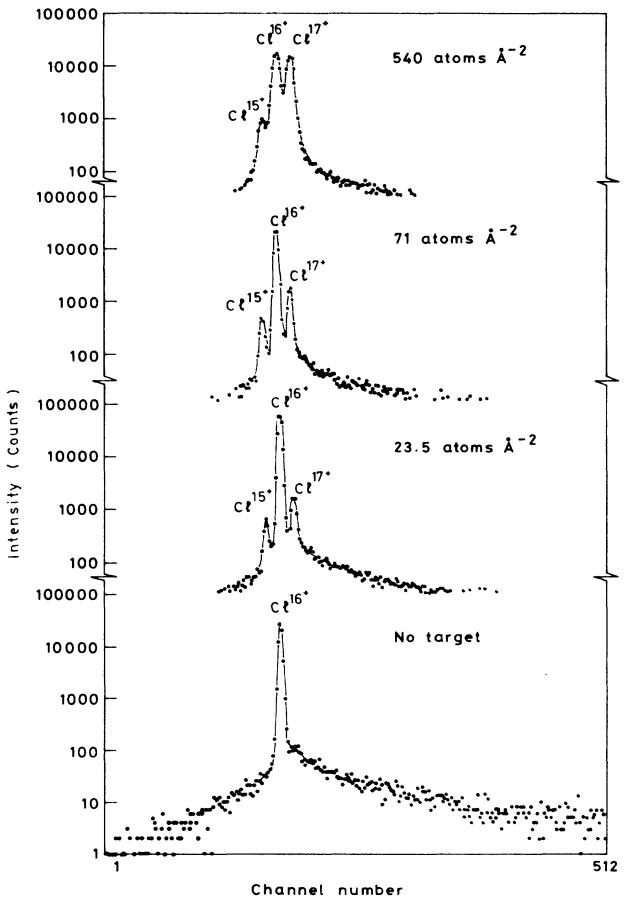

FIG. 2. Charge-state distributions for ^{35}Cl^{16+} incident on various thicknesses of target. The scale is logarithmic so one may see the small slit scattering background.

445±4 MeV. The final current was measured in a post-target Faraday cup. Electrical suppression of this cup was checked to assure reliable charge integration. Typically a few electrical nA of incident beam current could be obtained. Beam intensity levels could be reduced by defocussing lens $Q1$ such that about 10^3 counts/s were collected by the position sensitive detector (PSD) during charge-state measurements. Before measurements were made, a blank foil holder was placed in the beam path and the purity of the incident charge state including slit scattering was ensured. The slits prior to the electrostatic deflector plates were adjusted to give a suitable spatial extent to the deflected beam while minimizing background from scattering off these slits. Full details of the electrostatic deflector system are given elsewhere.[16] These adjustments thus present the C targets with a wide beam covering their 8-mm diameter which is then collimated by the slits at the entrance to the deflectors. Hence a sufficient sampling of the scattered distribution from the target was observed. Typical charge state spectra are shown in Fig. 2.

D. Spectroscopic observations

A complete determination of the population of all possible excited states of the H-like $^{35}Cl^{16+}$ and He-like $^{35}Cl^{15+}$ would require the detection of photons of wavelengths ranging from those produced by the Lyman transitions of $^{35}Cl^{16+}$ to those arising from Yrast decays for large n. The Bohr velocity matching criteria for projectile electron capture and the Born approximation for excitation suggested that only low-lying states would be significantly populated. Therefore, an x-ray energy range from about 2.5 to 4 keV was expected. For this purpose a thin (0.0003-in. Be) window Si(Li) detector of ~150-eV resolution was used. The detector was placed at 90° with respect to the beam direction with its center line parallel to the line of the foil. The detector was collimated by the 4-mm diameter of the Si(Li) crystal and a 4-mm-diam aperture about 8 mm in front of the detector. The Ly-α transition of $^{35}Cl^{16+}$ has a decay length of only about 1 μm at this beam energy. In order to detect all Ly-α light, targets mounted on the downstream side of the foil holder were tilted slightly (~2°).

With this collimation arrangement the detector viewed about 1.6 cm of the beam before significant shadowing occurred. Thus, decays from levels in the Lyman series as high as $n = 15-20$ could contribute most of their radiation to the observed spectra. These n values are sufficiently high to detect any significant cascading to lower levels.

Since the goal was to estimate the population of the various levels giving rise to the observed x-ray spectra, absolute efficiency of the Si(Li) detector system was determined. This was done by placing an ^{55}Fe source of known strength at the position of the target and measuring the resultant yield of $K\alpha$ and $K\beta$ x rays. This gave an absolute efficiency of $(1.48\pm0.01)\times10^{-4}$. The energy range of the calibration was extended to other energies using the known transmission efficiency of the Be window. The results were in reasonable agreement with calibrations published for similar detectors.[17] The resolution of the detector and Doppler broadening due to its finite aperture were estimated to provide a total resolution of about 160 eV. This is adequate to distinguish the Ly-α, Ly-β, Ly-γ, $2\,^1P-1\,^1S$, and $3\,^1P-1\,^1S$ transitions from one another.

A beam of Cl with selected charge-state ions was fo-

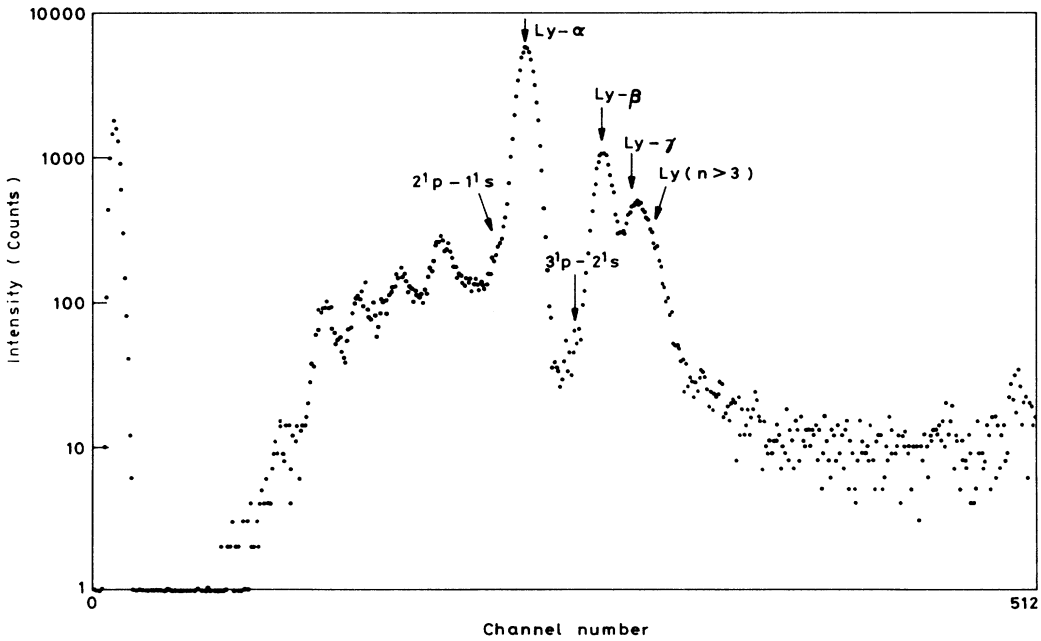

FIG. 3. Typical x-ray spectrum following interaction of $^{35}Cl^{17+}$ ions with a thin C foil (23.5 atoms/Å^2 C). Noting the logarithmic scale one sees that the hydrogenlike lines dominate this spectrum.

cused to ~3 mm diameter on the C foil. A minimum in the signal of Al $K\alpha$ x rays from the target holder served to indicate that a good quality beam transport has been achieved. The slits used upstream from the foils to define the beam were well shielded from the detector. Nuclear reactions and recoil ions from the target were negligible. Thus these sources of background could be disregarded. The charge-state fraction data along with the beam current measured in the Faraday cup were used to determine the total number of ions leaving the foil.

A typical x-ray spectrum obtained with $^{35}Cl^{17+}$ incident on a 23.5 atoms/Å^2 C foil is shown in Fig. 3. The Ly-α and Ly-β transitions are clearly resolved, while Ly-γ and other high-n value transitions are not. Some evidence of the $2\,^1P$-$1\,^1S$ line is present, but only very weakly as this case is far from charge-state equilibrium and very few $^{35}Cl^{15+}$ ions are formed. It is surmised that the background of x rays arises from bremsstrahlung, two-photon decay of $2S_{1/2}$, and x rays produced by scattered particles hitting the Al foil holder, giving rise to Al $K\alpha$ x rays, Si $K\alpha$ x rays, etc. (see Fig. 3). Radiative electron capture to the Cl K shell has an energy of about 11 keV. Although observed, it did not contribute to the background in the region of interest.

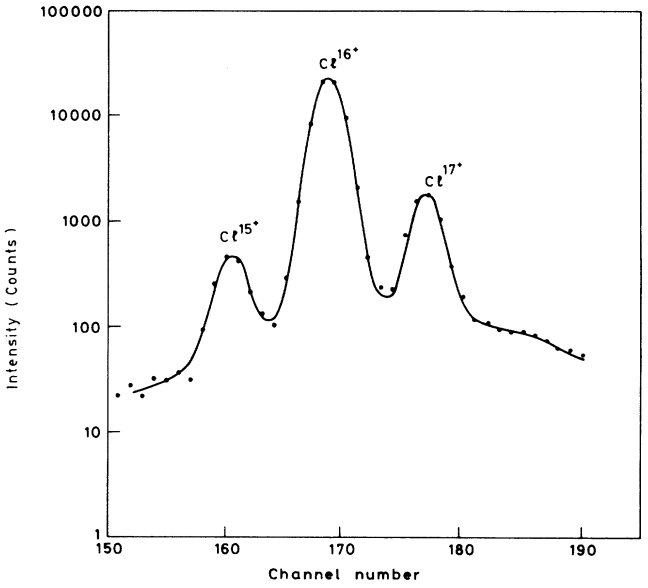

FIG. 4. Example of a calculated fit (continuous line) to charge-state distribution data (dots).

III. ANALYSIS OF DATA AND RESULTS

A. Charge-state distributions

Once charge-state distribution data for each C foil thickness had been obtained, there remained the problem of estimating the intensity of each charge-state fraction present. This required due care for two reasons. The spectra for the thinnest foils show a strong incident charge state peak, well separated from the small peaks of adjacent charge states. However, for these weakly populated charge states, the small amount of slit scattering background has to be carefully accounted for. In the case of the thicker foil data all the charge states that appeared strongly populated were broadened by multiple scattering. Thus account has to be taken of the overlap of the peaks of these charge states. In both cases the problem was solved by least-squares fitting appropriate shapes to the individual charge-state peaks and to the slit scattering background. First, the spectrum for each incident charge state without a foil present was used to test peak shape options. A Gaussian profile was found to give the best χ^2 minimum. The background for these spectra in the region either side of the incident charge state was equally well described either by a quadratic or exponential peak shape using the same χ^2 criteria. These peak shapes were then fitted to the data for each foil thickness allowing the peak position, width, and area as well as the background area to be determined by the χ^2 minimization program. An example of a fit to the data is shown in Fig. 4. The peak positions were found to match the zero foil positions for the appropriate charge state and their widths were equal for a given foil thickness. The peak widths were found to increase monotonically with foil thickness in a manner consistent with broadening due to multiple scattering. The area C_i of the line fitted to each charge state i was used to calculate charge-state fractions ϕ_i. The change in area that gave rise to a unit increase in the normalized χ^2 was taken as the standard error σ_i of the peak intensity.

The errors $\delta\phi_i^2$ on the charge-state fractions are then calculated from these estimates of σ_i via the relation

$$\phi_i = \frac{C_i}{C_1 + C_2 + \cdots + C_n} \,. \tag{3}$$

The additional error arising from foil thickness uncertainties are included in the error estimate for the ϕ_i as detailed by Woods.[14] The resultant charge state fractions ϕ_i and their error estimates are presented in Fig. 6 as a function of foil thickness.

B. Spectral line intensities

The determination of the spectral line intensities again required least-squares-fitting procedures, primarily because the detector system resolution of ~160 eV was not adequate to completely separate lines from all the transitions. Background subtraction required a reliable and consistent procedure. A Gaussian line shape was chosen *a priori* and found adequate for fitting to the various spectral lines which could be partially resolved. The Ly-γ and other Lyman lines are fitted with one line for Ly-γ and one for the rest. An adequate background description was achieved with a linear variation combined with several Gaussian lines of energy less than the $2\,^1P - 1\,^1S$ transition. The sensitivity of the background estimates in the region of the lines of interest to the linear choice was tested against choices of quadratic or exponential variations and found not to differ significantly. Figure 5 shows an example of the data and the fit to the various spectral lines. The relative positions of all the Gaussian lines

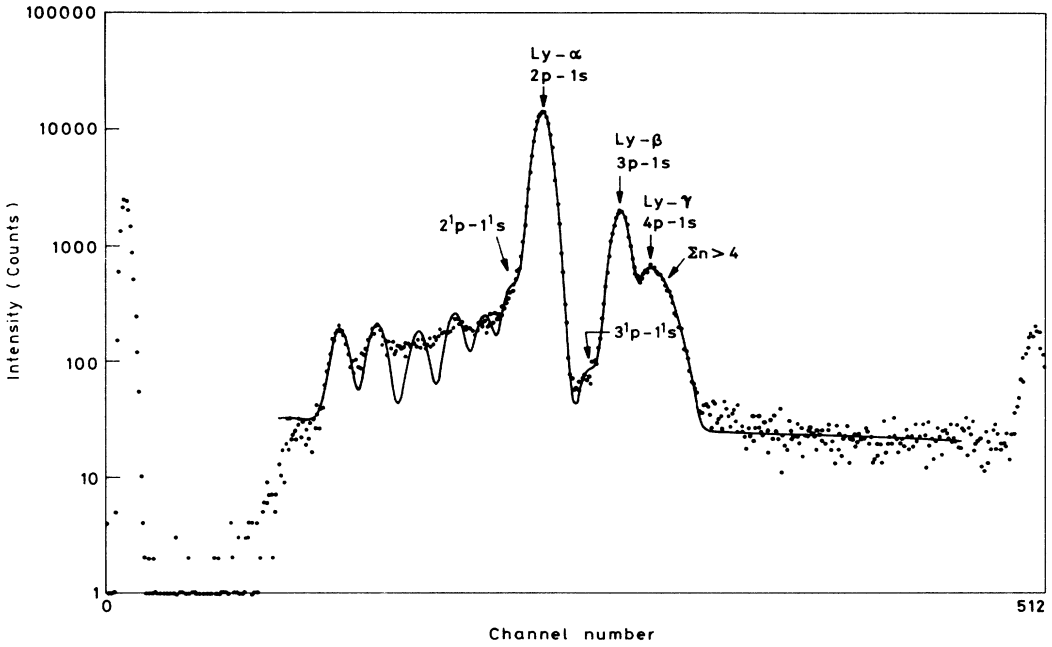

FIG. 5. Example of a calculated fit (continuous line) to the spectral intensity data (dots).

fitted to the spectra were found to agree with the relative positions expected from their known energies. The linewidth [full width at half maximum (FWHM)] of the fitted lines was also found to be in accord with the measured detector resolution and the estimate of Doppler broadening from the beam-foil source. Errors of the spectral line intensities were estimated in the same manner as described for the charge-state fitting procedure. These line intensities were then used with the detector efficiency calibration and assuming isotropic radiation to calculate absolute intensities with an additional error contribution from the detector calibration. These intensities give the number of ions formed in the upper state of the various transitions observed, including any cascades; since the length of beam viewed by the detector was relatively long compared to the decay length of the transitions observed. The excited-state fractions are then determined by dividing the absolute line intensities by the number of ions passing through the C foils. This latter quantity is calculated from the measured integrated charge and the average charge per ion determined from the charge state distributions. The cascade contribution decreases with excitation since the lifetime of such states also increases, we estimate that hydrogenic states of principal quantum number $n > 20$ should make a negligible contribution. We discuss the consequences of cascade errors to our cross-section estimates later. Previous observations of the $2\,^3S$ decay of 50-MeV Cl ions by Cocke *et al.*[18] imply a 1% $2\,^3S$ excited-state fraction. If we assume the population of $2\,^3S$ is in statistical equilibrium with $2\,^1P$ our data (Fig. 6) suggests a 5% $2\,^3S$ excited state fraction. We therefore neglect this possible systematic error in our $^{35}Cl^{15+}$ incident-beam data. Finally, excited-state fractions and their errors were calculated including foil thickness error estimates as before. The data so obtained are presented in Fig. 6 along with the charge-state fraction data.

C. Cross-section calculations

Before proceeding to a full cross-section analysis using Eqs. (1) it is important to examine the data obtained to determine how well it conforms to the assumptions used to design this experiment and achieve the conditions for such analysis. We wished to choose a ^{35}Cl ion energy (445 MeV) sufficiently high for the H-like and fully stripped Cl-ion fractions to dominate the equilibrium charge-state distribution; this is clearly the case as seen in Fig. 6. Only when charge state $^{35}Cl^{15+}$ is incident on the thin C foils do we observe a large fraction of $^{35}Cl^{15+}$ remaining after exit from the target. Therefore in the cases of $^{35}Cl^{16+}$ and $^{35}Cl^{17+}$ incident we expect negligible contributions from Auger rearrangement of doubly excited $^{35}Cl^{15+}$. When the $^{35}Cl^{15+}$ charge state fraction is large one would expect only a small portion of the beam to be doubly excited. This is reasonable when one considers that for the thinnest C foil double ionization of $^{35}Cl^{15+}$ produces only 0.2% $^{35}Cl^{17+}$. The $2\,^3S$ metastable state may be populated by the prestripper foil and survive to be a contaminant of the $^{35}Cl^{15+}$ incident beam. This state has a lifetime of approximately 170 ns. The corresponding decay length of 8.4 m is somewhat less than the distance from the prestripper to the chamber. We now examine the data of Fig. 6 plotted on a linear scale (Fig. 7) to determine whether or not single collision conditions [following Eq. (2)] have been achieved for any of the capture, loss, and excitation processes forming the charge-

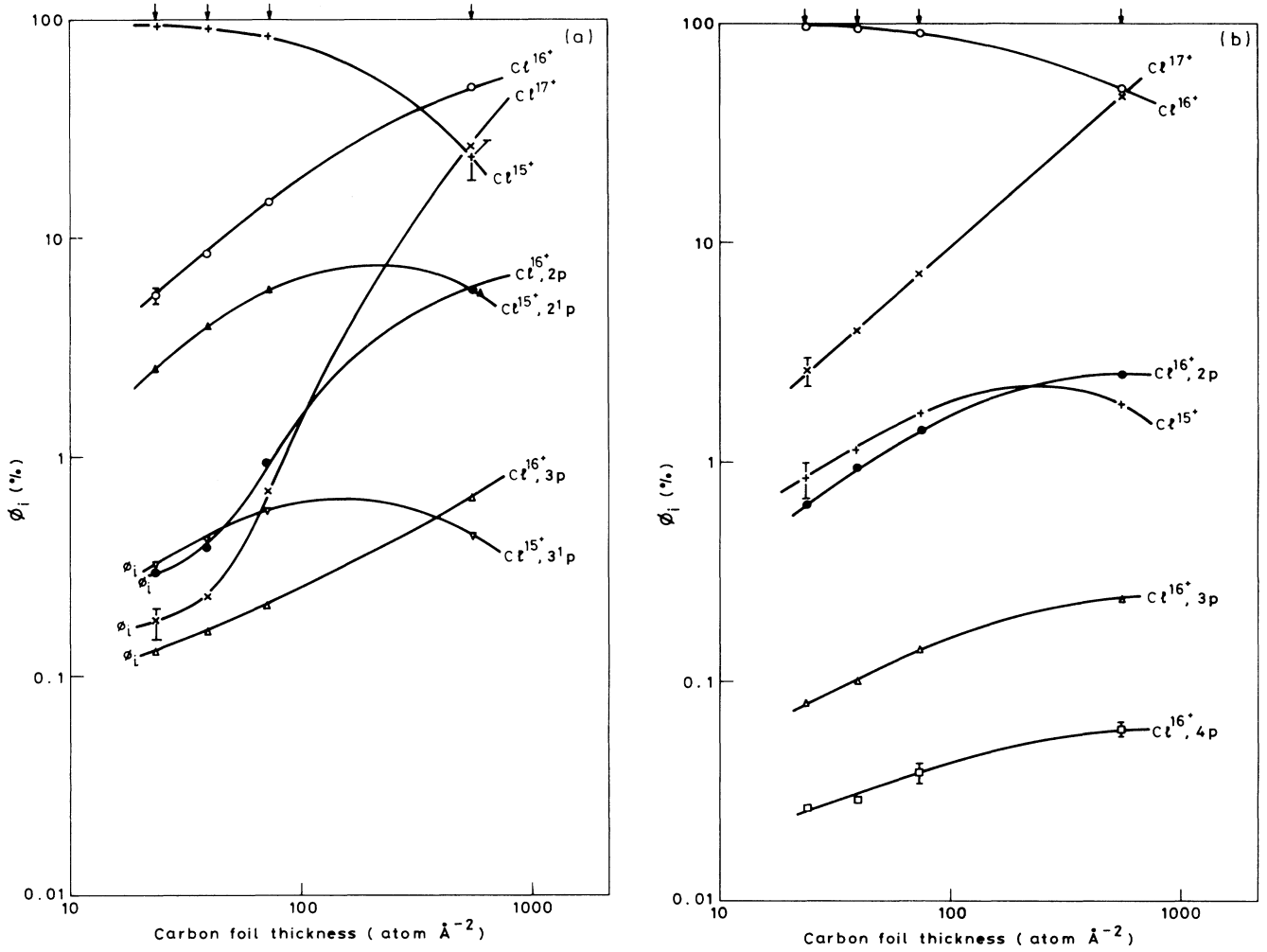

FIG. 6. Fractions of ions in various states versus carbon foil thickness for incident (a) $^{35}Cl^{15+}$, (b) $^{35}Cl^{16+}$, and (c) $^{35}Cl^{17+}$ ions. The lines through the data are nonlinear least-squares fits following solution of Eq. (1) as discussed in Sec. III C. For the thinnest foils the incident charge state is depleted by only a few percent giving charge-state distributions far from equilibrium.

state and excited-state fractions we have determined. Inspection of Fig. 7 indicates linear growth following Eq. (2) for electron capture by $^{35}Cl^{17+}$ to form $^{35}Cl^{16+}$, for ionization of $^{35}Cl^{16+}$ to $^{35}Cl^{17+}$, and for $^{35}Cl^{15+}$ to form $^{35}Cl^{16+}$ over the range of target thickness covered by the thinnest three carbon foils. In all other cases the curvature of the data is such that linear growth is met only for the thinnest two foils. The linear coefficient of least-squares parabolic fits to the data of Fig. 7 was therefore used in Eq. (2) to determine the cross sections given in Table I providing the parabolic term contribution was negligible for at least the thinnest two foils. The curvature seen in some of the data presented in Fig. 7 arises from, e.g., two-step processes such as $^{35}Cl^{16+} \rightarrow {}^{35}Cl^{16+}2p$ followed by $^{35}Cl^{16+}2p \rightarrow {}^{35}Cl^{17+}$, i.e., excited-state ionization.

A solution of Eq. (1) may provide estimates of some of the cross sections for the second-step processes which cannot be found by use of Eq. (2) as pure incident beams of, e.g., $^{35}Cl^{16+}$ $2p$ are not available. For this purpose we recast Eq. (1) in matrix notation $d\underline{\phi}/dx = S\underline{\phi}$ where

$$S\underline{\phi} = \begin{pmatrix} -\sum_{i+1} \sigma_{ij} & \sigma_{21} & \sigma_{31} \cdots \\ \sigma_{12} & & \\ \sigma_{13} & & \\ \vdots & & \end{pmatrix} \begin{pmatrix} \phi_1 \\ \phi_2 \\ \phi_3 \\ \vdots \end{pmatrix} .$$

The charge- and excited-state fractions ϕ_n included in ϕ are $^{35}Cl^{17+}$, $^{35}Cl^{16+}$, $^{35}Cl^{16+}2p$, $^{35}Cl^{16+}3p$, $^{35}Cl^{16+}4p$, $^{35}Cl^{15+}$, $^{35}Cl^{15+}2\,{}^1P$, $^{35}Cl^{15+}3\,{}^1P$. The $^{35}Cl^{16+}4p$ fraction is small ($\leq 0.1\%$) and includes possible unresolved components for $^{35}Cl^{16+}n$, $n > 4$. The cross sections σ_{ij} included in S are those connecting each of the ϕ_i to ϕ_j describing various processes of excitation, deexcitation, electron loss, and capture. This matrix equation is solved numerically using the technique described by Datz *et al.*[8] and based on standard nonlinear least-squares fitting.[19] A detailed description of these methods and the determination of errors on the calculated cross sections is given by Woods.[14] The cross sections so determined were in

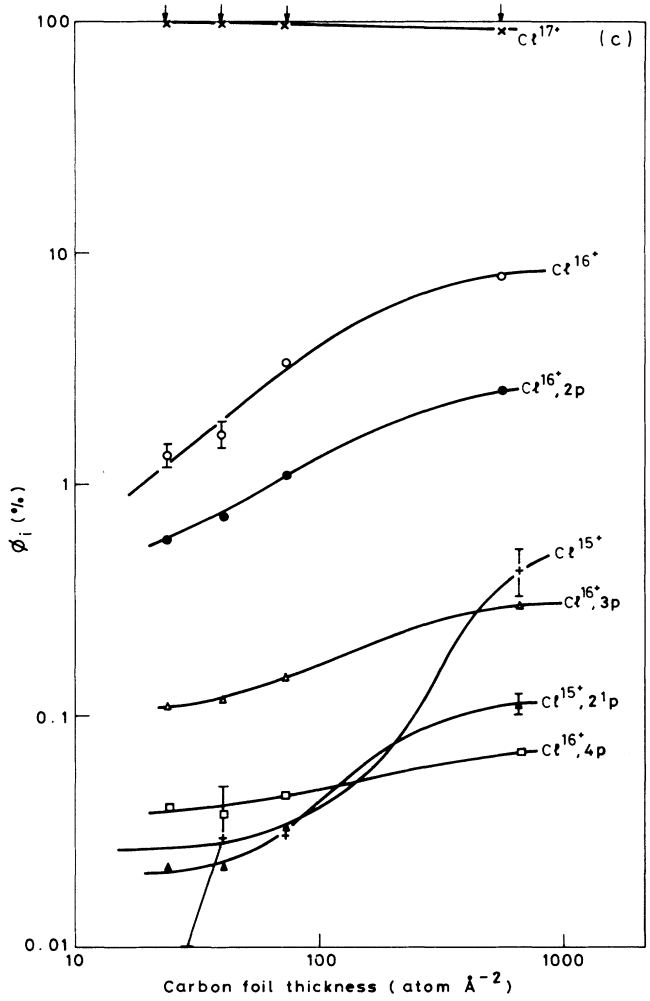

FIG. 6. (*Continued*).

agreement with those found using Eq. (2) within the errors of those values. A few additional cross sections were obtained primarily for the ionization of excited state $^{35}Cl^{16+}$; these are also given in Table I. Many cross sections were found to have zero values with, however, large uncertainties indicating that insufficient data was available to determine them, again a consequence of not having pure incident beams of excited-state ions.

Some of the estimates of the cross sections given in Table I contain systematic errors arising from the inclusion of cascade contributions to, e.g., $^{35}Cl^{16+}2p$, $^{35}Cl^{16+}3p$, $^{35}Cl^{15+}2\,^1P$ excited-state fractions. Following the method of Chetioui *et al.*[20] we can obtain an estimate of these errors for the $^{35}Cl^{16+}2p$ fraction. The cascade contribution of *ns* states ($n>2$) to the $^{35}Cl^{16+}2p$ fraction is negligible in the case of electron capture as all theories of capture predict small populations for these states.[20] We can estimate the $^{35}Cl^{16+}3d$ cascade contributions to $^{35}Cl^{16+}2p$ if we assume $^{35}Cl^{16+}3d$ is populated statistically relative to $^{35}Cl^{16+}3p$ measured. This assumption would on the basis of capture theory[20] and the data of Chetioui *et al.* lead to an overestimate for this cascade. As all of the $^{35}Cl^{16+}3d$ fraction deexcites via $^{35}Cl^{16+}2p$ we obtain ca. -20% [i.e., $-\sigma(^{35}Cl^{16+}3p)=0.6$] correction to the $\sigma(^{35}Cl^{17+}\rightarrow{}^{35}Cl^{16+}2p)$ capture cross section. Other cascades would be expected to increase this correction. However, we note that the $^{35}Cl^{16+}3p$ and $^{35}Cl^{16+}4p$ fractions are small relative to the $^{35}Cl^{16+}2p$ fraction; significantly smaller than the relative values obtained by Chetioui *et al.*[20] for the equivalent hydrogenic states of 400-MeV Fe ions for which the cascade correction to the $2p$ states was ca. -50%. The cascade corrections for the solid C target data we have obtained would be expected to be smaller than for a thin gas target such as Chetioui *et al.* used because the electron loss from excited-state fractions is expected to be larger in the solid target. These cascade corrections only affect the estimates of cross sections which populate the excited-state fractions; the rest of the cross sections, such as $^{35}Cl^{17+}$ to $^{35}Cl^{16+}$ total capture cross sections are free of this source of systematic errors.

IV. COMPARISON OF MEASURED CROSS SECTIONS WITH THEORY

Let us first examine the process of electron capture. There are several theoretical approaches to these calculations, some of these are very sophisticated in the use of

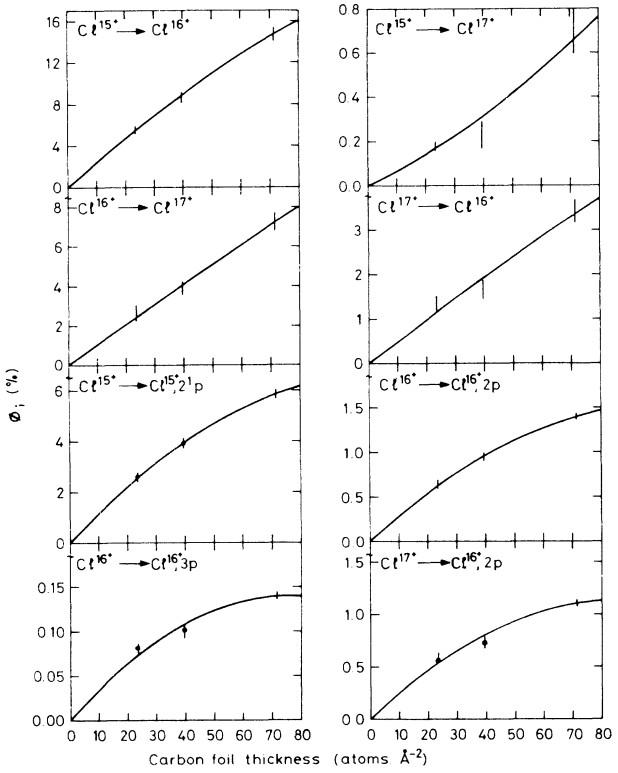

FIG. 7. Some of the data of Fig. 6 presented on a linear scale with parabolic fits to the data shown (continuous lines). The $^{35}Cl^{16+}$ to $^{35}Cl^{17+}$, i.e., electron-loss, data are linear as are the data for electron capture by the bare ion $^{35}Cl^{17+}$. The other data illustrated show varying degrees of curvature originating from two-step processes such as electron excitation from the ground state followed by ionization from the excited state (e.g., $^{35}Cl^{16+} \rightarrow {}^{35}Cl^{16+}3p$ followed by $^{35}Cl^{16+}3p \rightarrow {}^{35}Cl^{17+}$).

complicated numerical calculations such as the continuum distorted-wave method of Belkic and Gayet.[21] A method which does not require complicated calculations and which we have previously found to be satisfactory in a study of 36-MeV ^{12}C interacting with C targets[6] is examined here. The Eikonal or Glauber approximation[22] includes the interaction between the electron and the $^{35}Cl^{17+}$ projectile nucleus as does the OBK approximation.[23] In addition, the eikonal approximation also includes the interaction between the electron and the target nucleus to which it is bound via an eikonal phase factor in the final-state wave function. Since this interaction tends to retard the electron, a reduction in cross section over the OBK value is obtained. This approach has been developed for capture of $1s$ target electrons to principal projectile shells. An extension to projectile subshells (n,l) has also been given by Eichler and Chan,[24] and to other target shells of multielectron targets by Eichler.[25] We use this latest development embodied in Eichler's code[26] even though Ho *et al.*[27] have cast doubt on Eichler's treatment of multielectron targets. This form of Eichler's approximation contains a parameter Z_2' describing the effective screened target charge seen by the projectile and is described as providing the final-state interaction. If the capture occurs far away from the target nucleus then $Z_2' \simeq 1$ and if it captures within the target K shell then $Z_2' \simeq Z_2$. There is therefore some latitude in choosing Z_2'. We chose the value 3.5 for C targets, a value that coincidentally satisfied previous comparison with data for 36-MeV ^{12}C on C.[6] Eichler also treats screening in two other ways by introducing a factor θ to describe the reduction of the electron binding energy over the value given by its wave function $\varepsilon = \frac{1}{2}Z_2^2/n^2$, Eichler takes $\varepsilon = \theta Z_2^2/2n^2$, where $\theta \leq 1$. For a K electron $\theta = 0.642$ and for an L electron $\theta = 0.178$. The value of Z_2 is also chosen to take screening into account by the use of Slater's rule which for a carbon K electron $Z_2 = Z_n - 0.3$ and for L electrons $Z_2 = 3.25$, where Z_n is the nuclear charge. The theoretical values obtained using these parameters are given also in Table I for comparison. We are aware of no equivalent theoretical treatment for one-electron capture by $^{35}Cl^{16+}$ to form $^{35}Cl^{15+}$.

There is reasonable agreement between our fitted values and theory even though the variable parameters described above were chosen to match the data for 36-MeV $^{12}C^{6+}$ incident on C. From this study we conclude that this semiempirical capture theory can deal with a range of projectile charges from 6+ to 17+ and a velocity range of $\beta = v/c$ from about 0.018 to 0.2 for carbon targets with reasonable accuracy. We can estimate the $^{35}Cl^{16+}2p$ capture cross-section with the cascade contribution from $^{35}Cl^{16+}3d$ using the theoretical $\sigma(^{35}Cl^{17+} \rightarrow {}^{35}Cl^{16+}3d)$ cross section, a value of 5 is found, i.e., a 40% increase over the value of 3 for capture to the $^{35}Cl^{16+}2p$ fraction alone.

To treat electron loss and excitation we choose the Born approximation. The formulation of the Born approximation for complex targets with incident H-like ions in the $1s$ and the $2s$ states we choose is due to Gillespie.[28–30] Again this choice is made primarily because of its success in describing previous data for 36-MeV ^{12}C ions in C targets. His estimates are scaled by $6^2/Z_2^2$ as suggested by McDowell and Coleman.[31] The ionization cross sections for excited states were simply estimated by the Bohr[5] result $\sigma(n \rightarrow \infty) = n^2\sigma(1s \rightarrow \infty)$. The agreement between theory and experiment for electron loss $^{35}Cl^{16+} \rightarrow {}^{35}Cl^{17+}$ and $^{35}Cl^{16+}2p \rightarrow {}^{35}Cl^{17+}$ is within 30%. However, this agreement is worse (factor of 4) for electron excitation $^{35}Cl^{16+} \rightarrow {}^{35}Cl^{16+}2p$. There is of course a large number of cross sections for which we have determined fitted values but have no theory to compare.

V. SUMMARY AND CONCLUSION

This experiment was designed on the basis of an extrapolation of a previous study of 36-MeV ^{12}C ions incident on C targets,[6] using theory for electron capture, loss, and excitation that appeared satisfactory for that case. With 445-MeV ^{35}Cl ions traversing C targets we had hoped to achieve single collision conditions for some of the above processes for populating the $^{35}Cl^{17+}$, $^{35}Cl^{16+}$, and $^{35}Cl^{15+}$ ions using the thinnest C foils available. For thicker tar-

TABLE I. Cross sections determined from linear growth regime using Eq. (2) and also those additional cross sections obtained from nonlinear regime and solution of Eq. (1). Theoretical estimates described in the text are given for some of the cross sections measured.

Channel	Cross sections (10^{-20} cm^2) Measured	Theoretical
Cross sections determined from Eq. (2)		
$\sigma(^{35}Cl^{16+} \rightarrow {}^{35}Cl^{17+})$	10±2	18[a]
$\sigma(^{35}Cl^{15+} \rightarrow {}^{35}Cl^{16+})$	24±2	
$\sigma(^{35}Cl^{15+} \rightarrow {}^{35}Cl^{17+})$	0.63±1.3	
Electron capture		
$\sigma(^{35}Cl^{17+} \rightarrow {}^{35}Cl^{16+})$ for all n	5±1	8.4[b]
Electron excitation		
$\sigma(^{35}Cl^{16+} \rightarrow {}^{35}Cl^{16+}2p)$	3.1±0.4	12[a]
$\sigma(^{35}Cl^{16+} \rightarrow {}^{35}Cl^{16+}3p)$	0.38±0.007	2.2[a]
$\sigma(^{35}Cl^{15+} \rightarrow {}^{35}Cl^{15+}2\,{}^1P)$	12.2±1	
Additional cross sections determined from Eq. (1)		
Electron loss		
$\sigma(^{35}Cl^{16+}2p \rightarrow {}^{35}Cl^{17+})$	120±90	72[a]
$\sigma(^{35}Cl^{16+}3p \rightarrow {}^{35}Cl^{17+})$	300±100	
$\sigma(^{35}Cl^{15+} \rightarrow {}^{35}Cl^{14+})$	0.5±0.1	
Electron capture		
$\sigma(^{35}Cl^{17+} \rightarrow {}^{35}Cl^{16+}2p)$	2.8±0.4	3[b]
$\sigma(^{35}Cl^{17+} \rightarrow {}^{35}Cl^{16+}3p)$	0.6±0.2	1[b]
$\sigma(^{35}Cl^{16+} \rightarrow {}^{35}Cl^{15+}5n)$	3±0.5	

[a]Gillespie (Refs. 28–30).
[b]Eichler (Ref. 5).

gets we expected to reach a multiple collision regime. This was found to be the case.

The cross sections for total capture (e.g., $^{35}Cl^{17+} \rightarrow {}^{35}Cl^{16+}$, for all n) and electron loss from the ground state (e.g., $^{35}Cl^{16+} \rightarrow {}^{35}Cl^{17+}$) were as a result easily determined with a precision of ca. 20%. Cross sections involving an initial or final specific excited state were less well determined because pure incident beams of such ions were not available and recourse had to be taken to more complicated analysis of nonlinear growth. In addition, these cross sections suffered from a systematic error (we estimate ca. −20%) due to cascade contributions.

Agreement between theoretical predictions of Eichler's semiempirical electron-capture theory and our measured values are in reasonable accord given the somewhat arbitrary choice of theoretical parameters we have made.

Gillespie's Born approximation calculations for ionization of the ground state $^{35}Cl^{16+}$ ion is in accord with our experimentally determined value. However, the excitation cross section we have determined for $^{35}Cl^{16+}$ ground-state ions differ by about a factor of 4.

ACKNOWLEDGMENTS

We wish to acknowledge the help and encouragement of Dr. George Gillespie and Professor Jorg Eichler who kindly supplied a copy of his computer code for calculating capture cross sections. Support with target making from M. Miller was appreciated. The help with setting up and running of the data-acquisition system provided by W. T. Milner and J. A. Biggerstaff was welcome. The general helpfulness and encouragement of the HIRRF facility staff contributed to our pleasure and success in taking these data. Support for C. J. Sofield from the Underlying Programme of the UKAEA is gratefully acknowledged. This research was sponsored in part by the U.S. Department of Energy, Division of Chemical Science and the Office of Fusion Energy under Contract No. DE-AC05-84OR21400 with Martin Marietta Energy Systems, Inc. and in part under Contract No. DE-AC02-76ER02753 with Kansas State University. Travel grants were provided to L. B. Bridwell, P. L. Pepmiller, and C. J. Sofield by NATO.

[1]D. Belkic, R. Gayet, and A. Selin, Phys. Rep. **56**, 279 (1979).
[2]P. T. Greenland, Phys. Rep. **81**, 131 (1982).
[3]B. H. Bransden, in *Invited Papers of the Fifteenth International Conference on the Physics of Electronic and Atomic Collisions, Brighton, 1987*, edited by J. Geddes, H. B. Gilbody, A. E. Kingston, and C. J. Latimer (Queen's University, Belfast, 1987).
[4]E. Baron and W. B. Delaunay, Phys. Rev. A **12**, 40 (1975).

[5]N. Bohr, K. Danske Videnskab. Selsk. Mat.-Fys. Medd. **18** (8) (1948).
[6]C. J. Woods, C. J. Sofield, N. E. B. Cowern, M. Murrell, and J. Draper, J. Phys. B **17**, 867 (1984).
[7]S. K. Allison, Rev. Mod. Phys. **30**, 1137 (1958).
[8]S. Datz, N. O. Lutz, L. B. Bridwell, C. D. Moak, H. D. Betz, and L. D. Ellsworth, Phys. Rev. A **2**, 430 (1970).
[9]M. Nobes, J. Sci. Instrum. **42**, 753 (1965).
[10]Supplied by Chemical Concentrates Ltd., London.
[11]J. F. Ziegler, *Stopping Powers and Ranges in All Elemental Matter* (Pergamon, Oxford, 1977).
[12]C. J. Sofield, C. J. Woods, N. E. B. Cowern, L. B. Bridwell, J. M. Butcher, and J. M. Freeman, Nucl. Instrum. Methods **203**, 509 (1982).
[13]C. J. Sofield, L. B. Bridwell, N. E. B. Cowern, N. R. S. Tate, and D. W. L. Tolfree, Nucl. Instrum. and Methods **186**, 505 (1981).
[14]C. J. Woods, Ph.D. thesis, Oxford University, 1983; UKAEA-AERE Report No. 10795, 1983 (unpubished).
[15]H. D. Betz, Rev. Mod. Phys. **44**, 465 (1972).
[16]C. D. Moak, H. O. Lutz, L. B. Bridwell, L. C. Northcliffe, and S. Datz, Phys. Rev. **176**, 427 (1967).
[17]J. L. Campbell and P. L. McGhee, Nucl. Instrum. Methods **A248**, 393 (1968).
[18]C. L. Cocke, B. Curnette, and R. Randall, Phys. Rev. Lett. **31**, 502 (1973).
[19]P. R. Bevington, *Data Reduction and Error Analysis for the Physical Sciences* (McGraw-Hill, New York, 1969).
[20]A. Chetioui, K. Wohrer, J. P. Rozet, A. Jolly, C. Stephens, D. Belkic, R. Gayet, and A. Solin, J. Phys. B **16**, 3993 (1983).
[21]D. Belkic and R. Gayet, J. Phys. B **10**, 1923 (1977).
[22]R. J. Glauber, *Lectures in Theoretical Physics 1*, edited by W. E. Britten *et al.* (Interscience, New York, 1959).
[23]J. R. Oppenheimer, Phys. Rev. **31**, 349 (1928).
[24]J. K. M. Eichler and F. T. Chan, Phys. Rev. A **20**, 104 (1979).
[25]J. K. M. Eichler, Phys. Rev. A **23**, 498 (1981).
[26]J. K. M. Eichler (private communication).
[27]T. Ho, M. Lieber, K. T. Chan, and K. Omidvar, Phys. Rev. A **24**, 2933 (1981).
[28]G. H. Gillespie, Phys. Rev. A **16**, 943 (1977).
[29]G. H. Gillespie, Phys. Rev. A **18**, 1967 (1978).
[30]G. H. Gillespie, Phys. Rev. A **22**, 454 (1980).
[31]M. R. C. McDowell and J. P. Coleman, *Introduction to the Theory of Ion-Atom Collisions* (North-Holland, Amsterdam, 1970).